SLAC-PUB-2449
December 1979
(T/E)

THE INFLUENCE OF THE SELF-ENERGY DIAGRAMS ON THE SOLUTIONS OF A SCALAR BETHE-SALPETER EQUATION *

Bing An Li †
Stanford Linear Accelerator Center
Stanford University, Stanford, California 94305

Ting Chang Hsien
Institute of High Energy Physics, Academia Sinica
Beijing, People's Republic of China

Suh Yan, Tien Lun Chen, Ching Zhu Yang, Jing Fa Lu
Department of Physics, Nankai University
People's Republic of China

ABSTRACT

The influence of self-energy diagrams on solutions of the Bethe-Salpeter equation is studied by taking a $g\phi_1^*(x)\ \phi_1(x)\ \phi_2(x)$ interaction and under the ladder approximation. The results show that for ground state solutions, the self-energy diagrams will diminish the eigenvalues and alter the wave functions slightly. However for the excited states and anti-symmetric solutions, the influence of the self-energy diagrams is considerable, which completely alters the properties of the solutions. Their wave functions look like a δ-function and their eigenvalues are independent of the binding energy and the quantum numbers. The results also show that the infrared behavior of the self-energy diagrams is very important for the solutions of the equation. The results also show that the solutions from the ladder approximation are meaningful only in the loosely bound cases; as the binding becomes tight, the contribution from the self-energy diagrams becomes important.

(Sub. to Phys. Rev. D)

* Work supported in part by the Department of Energy under contract DE-AC03-76SF00515 and by the People's Republic of China.

† On leave of absence from the Institute of High Energy Physics, Beijing, People's Republic of China.

I. INTRODUCTION

During recent years interest in bound states has increased. We can use the Bethe-Salpeter equation to describe bound states. In general, the B-S equation becomes very complicated in the case of strong interactions. For example, the scalar B-S equation has the form

$$\Delta^{-1}(p_1)\ \Delta^{-1}(p_2)\ \chi(p) = \int G(P,p,p')\ \chi(p')\ d^4p' \tag{1.1}$$

where

$$(2\pi)^4\ \delta^4(p_1+p_2-P)\ \chi(p) = \int d^4x_1\ d^4x_2\ e^{-ip_1x_1\ -ip_2x_2} \times \langle 0|T\{\phi_1(x_1)\ \phi_1^*(x_2)\}|a\rangle \tag{1.2}$$

$$p_1 = p+\frac{P}{2}\ , \qquad p_2 = -p+\frac{P}{2}\ , \qquad \Delta^{-1}(p) = i(p^2+m^2)\ .$$

P_μ is the center of mass four momentum of the bound state. p_μ is the relative four momentum; m is mass of the particles (equal mass particles by assumption) which constitute the bound states. $G(P,p,p')$ is the integral kernel determined by four point irreducible Feynman diagrams as well as by self-energy diagrams. Up until now nobody has been able to add up all the diagrams in order to solve the equation. Thus some lower order diagrams are taken to solve the equation. A famous one is the ladder approximation.

In 1954, Wick[1] and Cutkosky[2] studied the solutions of a scalar B-S equation under the ladder approximation. Their results led to some understanding of the equation under this approximation. They found the existence of some abnormal solutions in the case of strong coupling. The abnormal states don't correspond to the solutions of the non-relativistic equation. The non-relativistic bound states are in three

dimensional space. The quantum numbers are the radial quantum number and the orbital angular momentum. However, relativistic bound states are in four dimensional space. The abnormal states correspond to the quantization of the fourth dimensional space-time. Many people have studied this problem.[3] There are some different points of view. But up to now there aren't any physical states which correspond to the abnormal solutions. R. Blankenbecler and R. Sugar[4] have discussed the importance of satisfying unitary conditions in the equation. M. J. Levine and Jon Wright[5,6] have resolved a scalar B-S equation. They found that in the inelastic region the unitary condition

$$\sigma_{tot} \geq \sigma_{elastic} \tag{1.3}$$

can be violated if only ladder graphs are taken in the integral kernel. But if the contribution of self-energy diagrams is taken then the unitary condition is satisfied in the inelastic scattering region. We know that if the unitary condition is violated some unphysical effects will appear.

In this paper we want to discuss what changes will occur in the bound state solutions if the self-energy diagrams are included in the integral kernel.

The paper is divided into six sections. In Section II we discuss the equation and the method used to solve the equation. In Section III the solutions without considering the contribution of self-energy diagrams are given and compared with those obtained by using other methods. In Section IV the solutions with self-energy diagrams are given. In Section V obtained wave functions are discussed. Section VI is a brief discussion of the results obtained by us.

II. THE EQUATION AND THE METHOD

For the sake of simplicity we still discuss a scalar B-S equation. The interaction is chosen to be

$$\mathcal{H}_i(x) = g\phi_1^*(x)\ \phi_1(x)\ \phi_2(x) \tag{2.1}$$

where $\phi_1(x)$ is a complex scalar field whose mass is denoted by m. $\phi_2(x)$ is a neutral scalar field whose mass is denoted by μ. The kernel G is taken up to second order diagrams in the coupling constant in Fig. 1. By using these diagrams (Fig. 1) the four point Green's function is denoted in Fig. 2. The bubbles of Fig. 2 are constituted by self-energy diagrams in Fig. 3.

With consideration of second order diagrams in the kernel, the integral kernel in the B-S equation has the following form

$$G(P,p,p') = \frac{i\lambda}{\pi^2}\ \frac{1}{(p-p')^2+\mu^2} - \lambda h(p)(p_1^2+m^2)(p_2^2+m^2)\ \delta^4(p-p') \tag{2.2}$$

where

$$h(p) = \int_{(m+\mu)^2}^{\infty} \frac{(p_1^2+m^2)\ \left[\sigma^2-(m+\mu)^2\right]^{\frac{1}{2}}\ \left[\sigma^2-(m-\mu)^2\right]^{\frac{1}{2}}}{\sigma^2(\sigma^2-m^2)^2\ (p_1^2+\sigma^2-i\varepsilon)}\ d\sigma^2$$

$$+ \int_{(m+\mu)^2}^{\infty} \frac{(p_2^2+m^2)\ \left[\sigma^2-(m+\mu)^2\right]^{\frac{1}{2}}\ \left[\sigma^2-(m-\mu)^2\right]^{\frac{1}{2}}}{\sigma^2(\sigma^2-m^2)^2\ (p_2^2+\sigma^2-i\varepsilon)}\ d\sigma^2 \tag{2.3}$$

The expression h(p) of the self-energy diagrams is obtained by using the method of the spectral function. The renormalization is considered.

Substituting formula (2.2) into Eq. (1.1) and after Wick rotation, the equation can be written in the following form

$$(p_1^2+m^2)(p_2^2+m^2)\chi(p) = \frac{\lambda}{\pi^2}\int \frac{\chi(p')\, d^4p'}{(p-p')^2+\mu^2} + \lambda h(p)(p_1^2+m^2)(p_2^2+m^2)\chi(p) \qquad (2.4)$$

Now both the momentum p and p' are in the Euclidean space. In the rest frame of the bound state, by using the rotation invariance of the equation, we single out the three dimensional harmonics corresponding to the orbital motion, and discuss the case in which the orbital quantum numbers are ℓ and m:

$$\chi(p) = \frac{1}{|\vec{p}|} f_\ell\,(|\vec{p}|, p_4)\, Y_{\ell m}(\theta,\phi) \quad . \qquad (2.5)$$

Substitute the formula (2.5) into Eq. (2.4) and we obtain

$$\psi_\ell(p) = \frac{2\lambda}{\pi}\int_{-\infty}^{+\infty} dp_4' \int_0^{\infty} d|\vec{p}'|\, \frac{Q_\ell(a)}{L(p)\, L(p')}\, \psi_\ell(|\vec{p}'|, p_4') + \lambda h(p)\psi_\ell(p) \quad , \qquad (2.6)$$

where $Q_\ell(a)$ is the Legendre function of the second kind and

$$a = \frac{(p_4 - p_4')^2 + |\vec{p}|^2 + |\vec{p}'|^2 + \mu^2}{2|\vec{p}|\ |\vec{p}'|} \quad ,$$

$$\psi_\ell(p) = L(p)\, f_\ell(p) \quad , \qquad (2.7)$$

$$L^2(p) = (|\vec{p}|^2 + p_4^2 + 1 - \eta^2)^2 + 4\eta^2 p_4^2$$

$$\eta = \frac{M}{2m}$$

M is the rest mass of the bound state, η is a related parameter which denotes the binding energy. All the quantities in Eq. (2.6) are in units of m, hence are dimensionless.

Equation (2.6) is a two-dimensional integral equation in the Euclidean space and is invariant under the transformation $p_4 \leftrightarrow -p_4$. Using this symmetry, the equation can be rewritten as

$$\psi_\ell^\pm(p) = \lambda h(p) \psi_\ell^\pm(p) + \lambda \int_0^\infty dp_4' \int_0^\infty d|\vec{p}'| K^\pm(p,p') \psi_\ell^\pm(p') \qquad (2.8)$$

where

$$K^\pm(p,p') = \frac{2}{\pi} \frac{Q_\ell[a(p_4)] \pm Q_\ell[a(-p_4)]}{L(p)\, L(p')} \qquad (2.9)$$

Because h(p) is an even function of the variable p_4, we have

$$\psi_\ell^\pm(|\vec{p}|,-p_4) = \pm \psi_\ell^\pm(|\vec{p}|,p_4) \qquad (2.10)$$

It is obvious that no non-relativistic approximation exists for $\psi_\ell^-(p)$; hence, it is the anomalous solution. In the following calculation, ψ_ℓ^+ and ψ_ℓ^- are solved separately.

Now introducing the following new variables:

$$|\vec{p}| = \frac{1+x}{1-x}, \quad p_4 = \frac{1+y}{1-y} \qquad (2.11)$$

then the regions of the integration of new variables x and y become (-1,1). The method of Gauss quadranture is used to discrete the integral equation and obtain a set of algebraic equations

$$\lambda^{-1} \chi_{ij}^\pm = h_{ij} \chi_{ij}^\pm + \sum_{\ell,m=1}^{N} A_{ij,\ell m} \chi_{\ell m}^\pm \qquad (2.12)$$

where

$$A^{\pm}_{ij,\ell m} = \frac{2\sqrt{\omega_i\omega_j\omega_\ell\omega_m}}{(1-x_i)(1-y_j)(1-x_\ell)(1-y_m)}\, k^{\pm}_{ij,\ell m}$$

$$\chi^{\pm}_{ij} = \frac{\sqrt{\omega_i\omega_j}}{(1-x_i)(1-y_j)}\, \psi^{\pm}_{ij} \qquad (2.13)$$

ω_i are the weights of Gaussian integration. Equation (2.12) is a set of coupled algebraic equations which is solved on a DJS-8 computer numerically.

III. THE SOLUTIONS WITHOUT CONSIDERING THE SELF-ENERGY DIAGRAMS

In order to examine the influence of the self-energy diagrams on the solutions and check the method used to solve the equation, we first solve the equation without considering the self-energy diagrams. After removing the self-energy diagram's term h(p) from Eq. (2.8), the equation becomes a standard Fredholm integral equation whose properties are well known. In the corresponding algebraic equation (2.12), after removing the term corresponding to the self energy diagrams, we use ten Gaussian points and solve the eigenvalues and eigenfunctions of a 100 × 100 determinant. The parameters η and μ are taken to be

$$\eta = 0.0,\ 0.2,\ 0.4,\ 0.6,\ 0.9,\ 0.99;$$

$$\mu = 1,\ 0.1,\ 0.01.$$

and the symmetric and anti-symmetric ground states and several excited states are solved for the S- and p- waves. The eigenvalues for $\mu = 1$ are shown in Table I, in which $\lambda^{\pm}_{\ell,n}$ are the eigenvalues corresponding to the symmetric and anti-symmetric wave functions with the orbital angular

momentum ℓ and quantum number n respectively, where n is labeled according to the magnitude of the eigenvalues from 0 on. The λ^*'s are obtained by Zin Linden[7] by expanding the wavefunction in the four-dimensional spherical harmonics and solving the resultant one dimensional integral equation by using 32 Gaussian points. From Table I we see that λ^* agree with $\lambda^+_{0,0}$ obtained by us up to the third effective figure. In paper[8] A. Pagnamenta solved the equation (without self-energy diagrams) by using 12 Gaussian points and obtained $\lambda^+_{0,0} = 3.4182$ (for $\eta = 0.0$), which agree with our result also up to the third effective figure. In paper[9] Schwartz exploited the variation method to calculate $\lambda^+_{0,1}$, $\lambda^+_{1,0}$ and $\lambda^-_{0,0}$, and his results agree with ours up to the second or third effective figure. The eigenvalues corresponding to $\mu = 0.1$ and 0.01 are given in Tables 2 and 3, from which we see that for fixed η, λ decreases as μ decreases; i.e., the spectrum of λ becomes denser as μ decreases. In order to examine the stability of the results obtained, we have also used eight Gaussian points to solve the equation and compared the results with the above mentioned ones in various references. It turns out that the eigenvalues tabulated in these tables remain unchanged up to the third effective figure for the ground state, and up to the second or third effective figure for the excited states.

IV. THE INFLUENCE OF THE SELF-ENERGY DIAGRAMS

When the self-energy diagrams are taken into consideration, we have to solve Eq. (2.21), which contains the following diagonal terms

$$h_{ij}\, \chi^{\pm}_{ij} \quad .$$

In solving the equation, ten Gaussian points are still used. The eigenvalues obtained are given in Tables 4, 5 and 6.

From these results we conclude that:

1. For $\mu = 1$, there exists a ground state solution of the symmetric wave function, corresponding eigenvalues are lower than that when the contribution of the self-energy diagram is neglected (30% lower for $\eta = 0$). This difference diminishes as η increases, and for $\eta \to 1$. They approach the same limit which shows that the contribution of the self-energy diagrams are small for loosely bounded states ($\eta \sim 1$). This can also be seen from Fig. 4. This result agrees with R. Blankenbecler and M. J. Levine[5,6].

2. For $\mu = 1$, all anti-symmetric solutions and symmetric excited solutions are degenerate and the eigenvalues are independent of η. In this case the calculating results show that

$$h(p)\ \chi(p) \quad >> \quad \frac{1}{\pi^2}\ \frac{1}{\left(p_1^2+1\right)\left(p_2^2+1\right)}\ \int\ \frac{\chi(p')\ d^4p'}{(p-p')^2+\mu^2}$$

Hence the contribution of the self-energy diagrams is dominant. In this case the eigenvalues are equal to the inverse of the maximum of h(p). For $\mu = 1$, we obtain

$$h(p)_{max} \quad = \quad 0.417 \quad = \quad \lambda^{-1}$$

Then

$$\lambda \quad = \quad 2.39 \quad .$$

It is the same with calculating results. As the term of the self-energy diagrams control the solution of the equation, the discrete spectrum doesn't exist and only the continuing spectrum exists. For the ground state of the anti-symmetric wave function its integral kernel K^- is small which causes the larger value $\lambda^-_{0,0} = 16.33$ in the case without considering self-energy diagrams. For the excited states of both symmetric and

anti-symmetric wave functions there are some zero points in the wave functions which cause the integration

$$\int \frac{\chi(p')\, d^4p'}{(p-p')^2+\mu^2} \quad , \qquad \text{for the excited states}$$

to be small which can be seen from the large values of $\lambda^{+}_{0,1}$, $\lambda^{+}_{0,2}$, $\lambda^{+}_{1,0}$, $\lambda^{+}_{1,1}$, $\lambda^{+}_{1,2}$, $\lambda^{-}_{1,0}$, $\lambda^{-}_{1,0}$ and $\lambda^{-}_{1,1}$ (Table 1). These results show that the integrations are small in the case of the ground state of the anti-symmetric wave function and the excited states. Thus as the self-energy term exists it will control the solution of the equation in these cases.

3. For $\mu = 0.1$ and 0.01 all the eigenvalues of the ground state corresponding to $\eta \leq 0.9$ are constant, i.e., $1 / h_{max}$. Only for loosely bounded states ($\eta > 0.99$) can the different eigenvalues be found and the ground state of the symmetric wave function exist. These eigenvalues approach the values without considering self-energy diagrams. The calculating results show that as μ is getting smaller the h(p) values are getting larger.

4. From Tables 5 and 6 we see that as parameter μ is getting smaller the corresponding eigenvalues are also smaller because the h(p) values are getting larger as μ decreases.

These results are shown in Figs. 4, 5, 6 and 7. From them we can see that the influence of the self-energy diagrams is considerable.

V. WAVE FUNCTIONS

The symmetric wave functions of the ground state $\psi^{+}_{0,0}(|\vec{p}|, p_4)$ for $\mu = 1$, $\eta = 0$ and $\eta = 0.99$ and anti-symmetric wave functions $\psi^{-}_{0,0}(|\vec{p}|, p_4)$ for

$\mu = 1$, $\eta = 0$ are shown in Fig. 8 where both cases of neglecting and considering the contribution from the self energy diagrams are included.

1. In Fig. 8 the dot-dash line represents the wave function $\psi^{+}_{0,0}$ corrected by the self-energy diagrams ($\mu = 1$, $\eta = 0$). This correction diminishes the eigenvalues from $\lambda^{+}_{0,0} = 3.14$ to $\lambda^{+}_{0,0} = 2.01$. But it can be seen from Fig. 8 that the correction to the shape of the wave function is small. Moreover, this correction becomes smaller as η increases. For $\eta = 0.99$ (Fig. 9) $\psi'^{+}_{0,0}$ having the contribution from the self-energy diagrams and $\psi^{+}_{0,0}$ without the self-energy diagrams are close to the same. The correction of the self-energy diagrams on the shape of the wave functions is much smaller for the ground state of the symmetric state.

2. Figure 10 represents the anti-symmetric wave function $\psi^{-}_{0,0}$ of the ground state without considering the correction by the self-energy diagrams ($\mu = 1$, $\eta = 0$). The behavior of the wave functions is very smooth. We cannot find any strange behavior comparing it with the wave function $\psi^{+}_{0,0}$.

3. Figure 11 represents the eigenvector $\chi^{-}_{0,0}$ (Fig. 10) by the formula (2.13). After the correction by the self-energy diagrams, $\chi^{-}_{0,0}$ changes into a δ-function-like solution, as shown in the upper right corner of Fig. 11. The central position of $\chi^{-}_{0,0}$ is just at that h(p) takes the maximum. In this case the self-energy diagrams are dominant in the equation.

VI. CONCLUSION

1. As $\eta \to 1$ the eigenvalues λ approach a same limit in the cases without self-energy diagrams and in those having the self-energy diagrams

for the symmetric ground state. The self-energy diagrams are not important for the loosely bound state and the ladder approximation is better in this case.

2. The influence of the self-energy diagrams on the shape of the wave fuction of the symmetric ground state is small. But the influence on the eigenvalues of the symmetric ground state is large in a tightly binding region.

3. The influence of the self-energy diagrams on the abnormal states and excited states is very large. Their eigenvalues are independent of η and the state's quantum number. The wave function looks like a δ-function. Going to the configuration space such distributions cannot correspond to a normal bound state.

4. The parameter μ is related to the infrared behavior of the self-energy diagrams. As μ is getting smaller the contribution of the self-energy diagrams is getting large. For $\mu = 1$ there exists a symmetric ground state in all η values. But for $\mu = 0.1$ and 0.01 it is only as $\eta > 0.99$ that the symmetric ground state exists.

5. The equation without self-energy diagrams is a standard Fredholm integral equation. But the equation having self-energy diagrams is not. The general B-S equation can be written as

$$\chi(p) = A(p)\,\chi(p) + \int G\,(P,p,p')\,\chi(p')\,d^4p' \qquad (6.1)$$

The function A(p) denotes the contribution of all the self-energy diagrams and G denotes all the four point irreducible Feynman diagrams. In this paper only the simplest case is discussed. In general, the equation is very complicated. But the results obtained by us show that the balance

between the two terms is needed in order to obtain a physical solution. In the configuration space the term of the self-energy diagrams represents the nonlocal interactions. In the case of the strong interaction the nonlocal interaction is important.

ACKNOWLEDGMENTS

We would like to thank Professor S. Drell, R. Blankenbecler, Y. S. Tsai and Dr. Bing-ren Li for their helpful discussions.

This work was supported in part by the Department of Energy under contract DE-AC03-76SF00515 and by the People's Republic of China.

REFERENCES

1. G. C. Wick, Phys. Rev. 96, 1124 (1954).
2. R. E. Cutkosky, Phys. Rev. 96, 1135 (1954).
3. Noboru Nakanishi, Supplement of the Progress of Theoretical Physics 43, 1 (1969).
4. R. Blankenbecler and R. Sugar, Phys. Rev. 142, 1051 (1966).
5. M. J. Levine and Jan Wright, Phys. Rev. 154, 1433 (1967).
6. M. J. Levine and Jan Wright, Phys. Rev. 157, 1416 (1967).
7. Zur Linden and Mitter, Nuovo Cimento 61B, 389 (1969).
8. A. Pagnamenta, Nuovo Cimento 53, 30 (1968).
9. Schwartz, Phys. Rev. 137, 717 (1965).

TABLE 1 ($\mu = 1$)

η	0.0	0.2	0.4	0.6	0.9	0.99
$\lambda^{+}_{0,0}$	3.416	3.342	3.114	2.717	1.665	1.010
λ^{*}	3.419	3.344	3.115	2.718	1.665	1.014
$\lambda^{+}_{0,1}$	16.69	16.40	15.52	13.90	9.79	7.07
$\lambda^{+}_{0,2}$	45.02	44.44	42.67	39.41	29.72	23.04
$\lambda^{+}_{1,0}$	16.30	16.02	15.17	13.68	9.80	7.73
$\lambda^{+}_{1,1}$	46.18	45.57	43.51	39.89	30.43	25.05
$\lambda^{+}_{1,2}$	85.82	85.07	82.81	79.01	68.17	59.16
$\lambda^{-}_{0,0}$	16.33	16.20	15.80	15.12	13.51	12.87
$\lambda^{-}_{0,1}$	46.45	46.09	44.98	43.09	38.60	36.79
$\lambda^{-}_{1,0}$	73.82	72.97	70.35	65.60	51.71	42.21
$\lambda^{-}_{1,1}$	109.4	108.4	106.4	102.3	91.13	84.91

TABLE 2 ($\mu = 0.1$)

η	0.0	0.2	0.4	0.6	0.9	0.99
$\lambda^{+}_{0,0}$	2.008	1.946	1.757	1.434	0.608	0.185
$\lambda^{+}_{0,1}$	6.04	5.85	5.28	4.31	1.86	0.63
$\lambda^{+}_{0,2}$	11.65	11.38	10.55	9.00	3.79	1.40
$\lambda^{+}_{1,0}$	5.95	5.76	5.20	4.22	1.82	0.61
$\lambda^{+}_{1,1}$	11.56	11.19	10.10	8.31	3.64	1.29
$\lambda^{+}_{1,2}$	17.60	17.30	16.38	13.59	6.35	2.42
$\lambda^{-}_{0,0}$	5.93	5.81	5.45	4.81	3.08	2.19
$\lambda^{-}_{0,1}$	11.55	11.31	10.59	9.29	5.69	3.95

TABLE 3 ($\mu = 0.01$)

η	0.0	0.2	0.4	0.6	0.9	0.99
$\lambda^{+}_{0,0}$	1.830	1.773	1.598	1.296	0.525	0.111
$\lambda^{+}_{0,1}$	4.88	4.72	4.24	3.42	1.31	0.22
$\lambda^{+}_{0,2}$	7.29	7.14	6.68	5.55	1.98	0.39
$\lambda^{+}_{1,0}$	4.68	4.53	4.06	3.26	1.24	0.23
$\lambda^{+}_{1,1}$	7.86	7.62	6.91	5.64	2.11	0.31
$\lambda^{+}_{1,2}$	9.02	8.83	8.28	7.08	2.51	0.56
$\lambda^{-}_{0,0}$	4.44	4.35	4.05	3.51	1.92	0.67
$\lambda^{-}_{0,1}$	7.45	7.29	6.77	5.74	2.86	0.88
$\lambda^{-}_{1,0}$	9.01	8.82	8.22	7.01	3.23	0.86

TABLE 4 ($\mu = 1$)

η	0.0	0.2	0.4	0.6	0.9	0.99
$\lambda'^{+}_{0,0}$	2.282	2.262	2.196	2.053	1.484	0.97
$\lambda'^{+}_{0,1}$	2.39	2.39	2.39	2.39	2.39	2.39
$\lambda'^{+}_{0,2}$	2.40	2.40	2.40	2.40	2.40	2.40
$\lambda'^{-}_{0,0}$	2.39	2.38	2.37	2.38	2.37	2.37
$\lambda'^{\pm}_{1,0}$	2.39	2.39	2.39	2.39	2.39	2.39

TABLE 5 ($\mu = 0.1$)

η	0.0	0.2	0.4	0.6	0.9	0.99
$\lambda'^{+}_{0,0}$	0.3317	0.3317	0.3317	0.3317	0.3317	0.1714
$\lambda'^{+}_{0,1}$	0.332	0.332	0.332	0.332	0.332	0.332

TABLE 6 ($\mu = 0.01$)

η	0.0	0.2	0.4	0.6	0.9	0.99
$\lambda'^{+}_{0,0}$	0.1378	0.1378	0.1378	0.1378	0.1378	0.0889
$\lambda'^{+}_{0,1}$	0.1378	0.1378	0.1378	0.1378	0.1378	0.1378
$\lambda'^{-}_{0,0}$	0.1378	0.1378	0.1378	0.1378	0.1378	0.1378
$\lambda'^{-}_{0,1}$	0.1379	0.1379	0.1379	0.1379	0.1379	0.1379

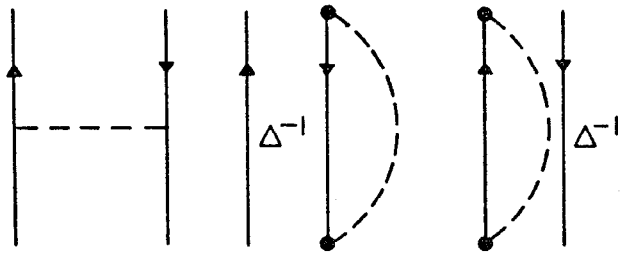

12 – 79 3749A1

Fig. 1

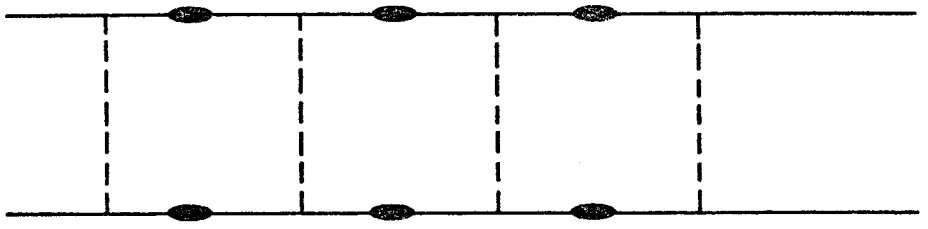

12 – 79 3749A2

Fig. 2

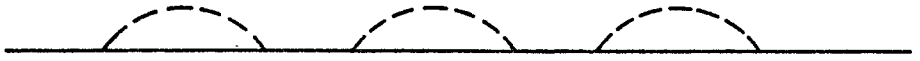

12 – 79 3749A3

Fig. 3

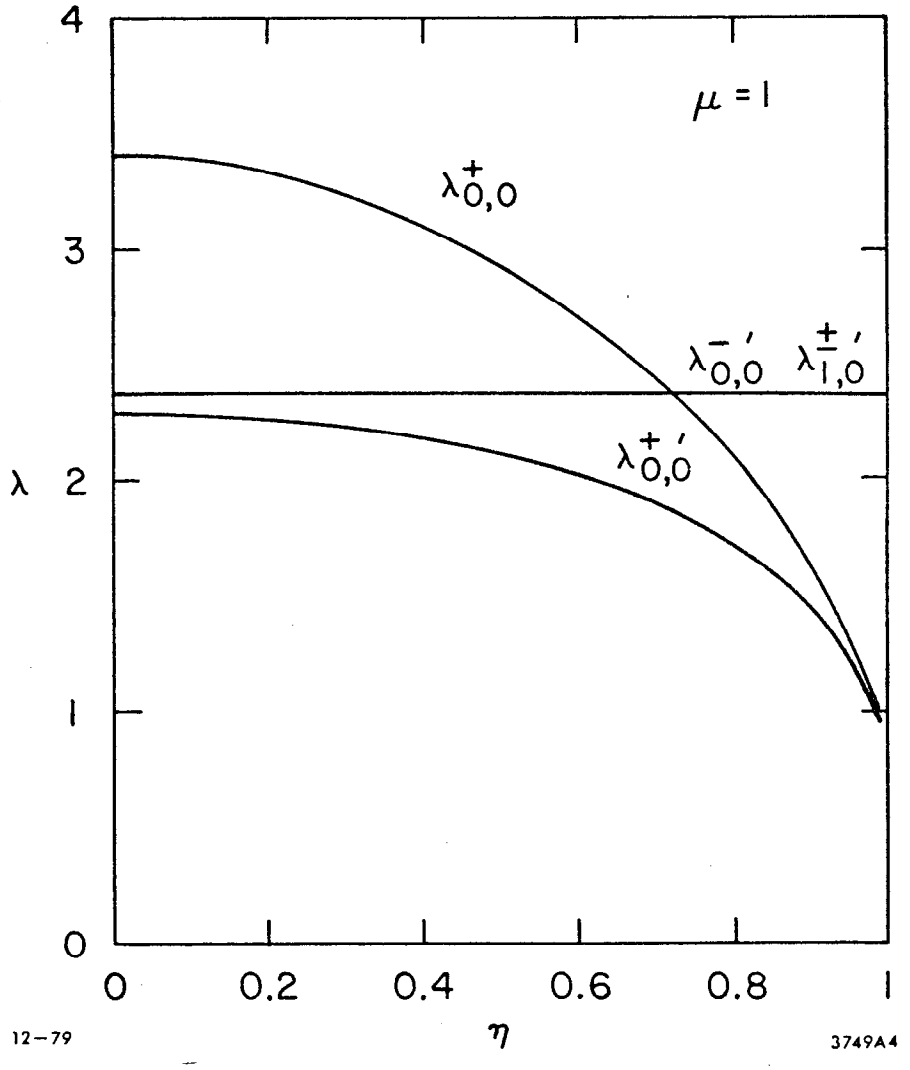
4
3
2
1
0
λ
μ = 1
$\lambda^{+}_{0,0}$
$\lambda^{-\prime}_{0,0}$
$\lambda^{\pm\prime}_{1,0}$
$\lambda^{+\prime}_{0,0}$
0
0.2
0.4
0.6
0.8
1
η
12-79
3749A4

Fig. 4

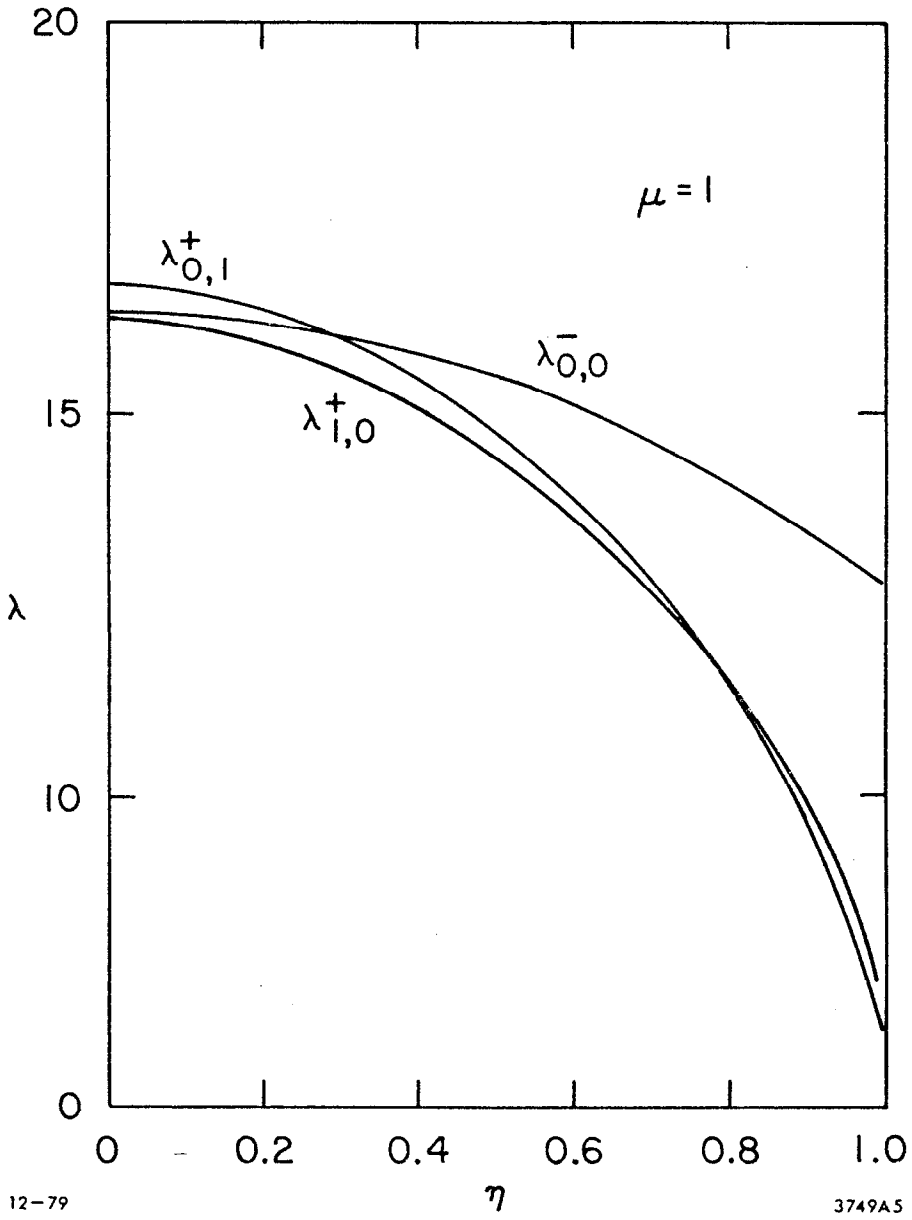
20
15
10
0
λ
μ = 1
$\lambda^{+}_{0,1}$
$\lambda^{-}_{0,0}$
$\lambda^{+}_{1,0}$
0
0.2
0.4
0.6
0.8
1.0
η
12-79
3749A5

Fig. 5

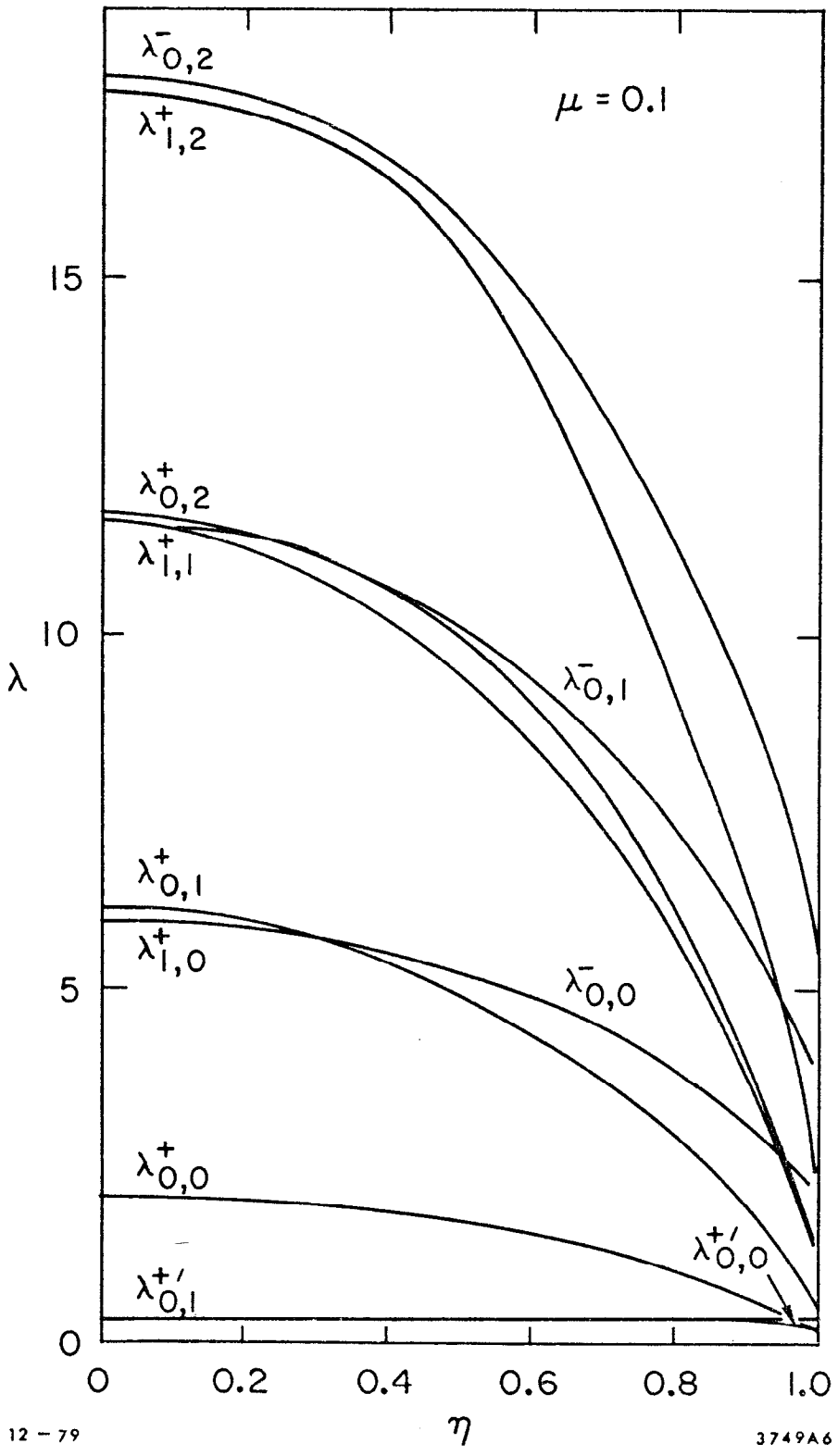
$\lambda^-_{0,2}$
$\lambda^+_{1,2}$
$\mu = 0.1$
15
$\lambda^+_{0,2}$
$\lambda^+_{1,1}$
10
λ
$\lambda^-_{0,1}$
$\lambda^+_{0,1}$
$\lambda^+_{1,0}$
5
$\lambda^-_{0,0}$
$\lambda^+_{0,0}$
$\lambda^{+\prime}_{0,0}$
$\lambda^{+\prime}_{0,1}$
0
0
0.2
0.4
0.6
0.8
1.0
η
12 – 79
3749A6

Fig. 6

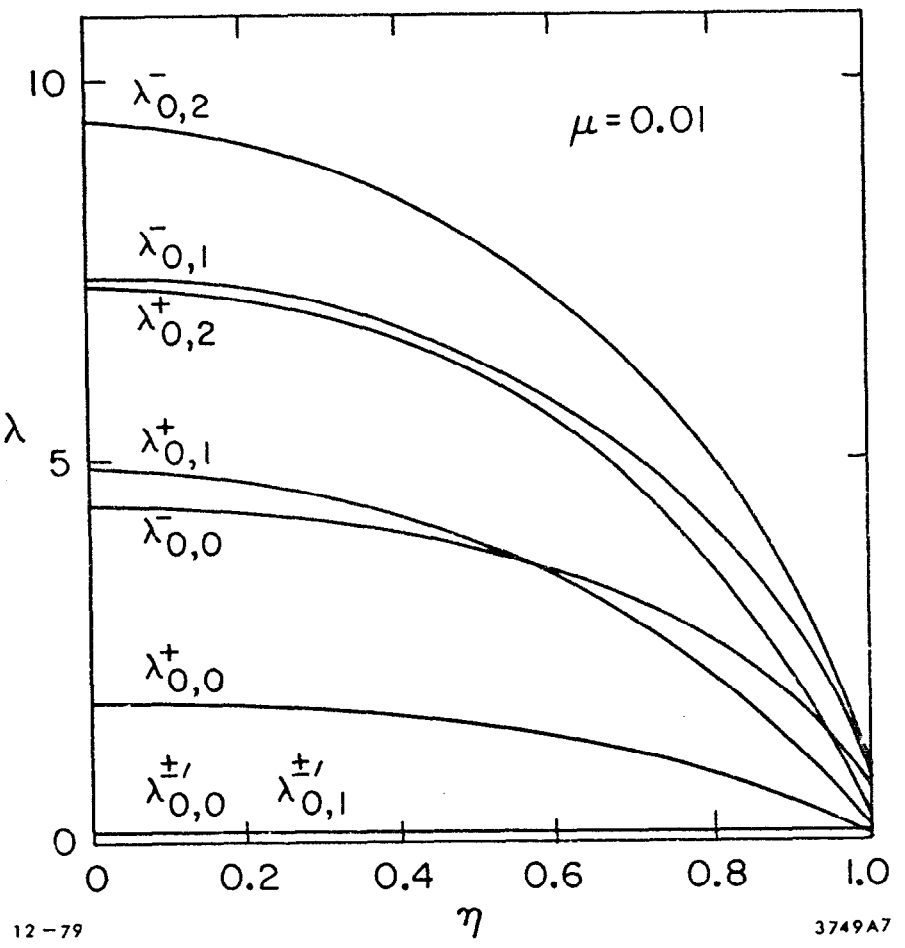
10
5
0
λ
$\lambda^{-}_{0,2}$
$\mu = 0.01$
$\lambda^{-}_{0,1}$
$\lambda^{+}_{0,2}$
$\lambda^{+}_{0,1}$
$\lambda^{-}_{0,0}$
$\lambda^{+}_{0,0}$
$\lambda^{\pm\prime}_{0,0}$
$\lambda^{\pm\prime}_{0,1}$
0
0.2
0.4
0.6
0.8
1.0
η
12 – 79
3749A7

Fig. 7

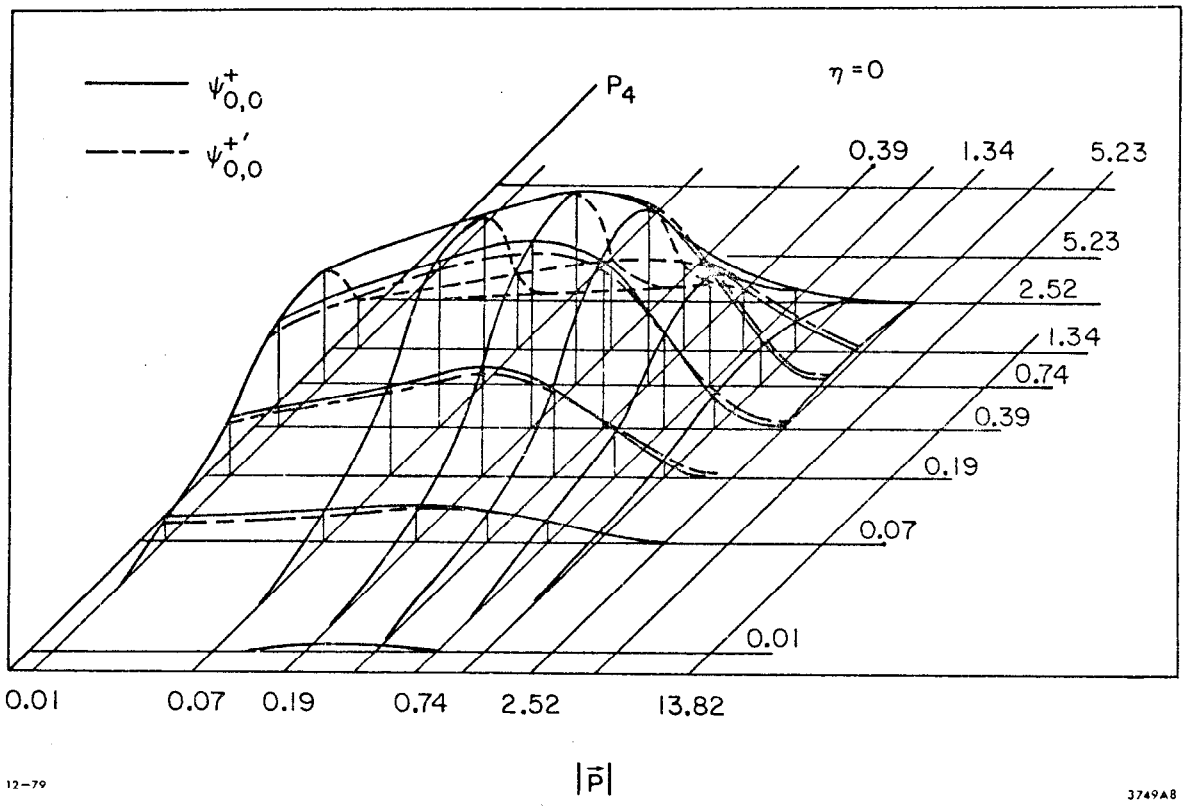
$\psi^{+}_{0,0}$
$\psi^{+\prime}_{0,0}$
P_4
$\eta = 0$
0.39
1.34
5.23
5.23
2.52
1.34
0.74
0.39
0.19
0.07
0.01
0.01
0.07
0.19
0.74
2.52
13.82
$|\vec{P}|$
12-79
3749A8

Fig. 8

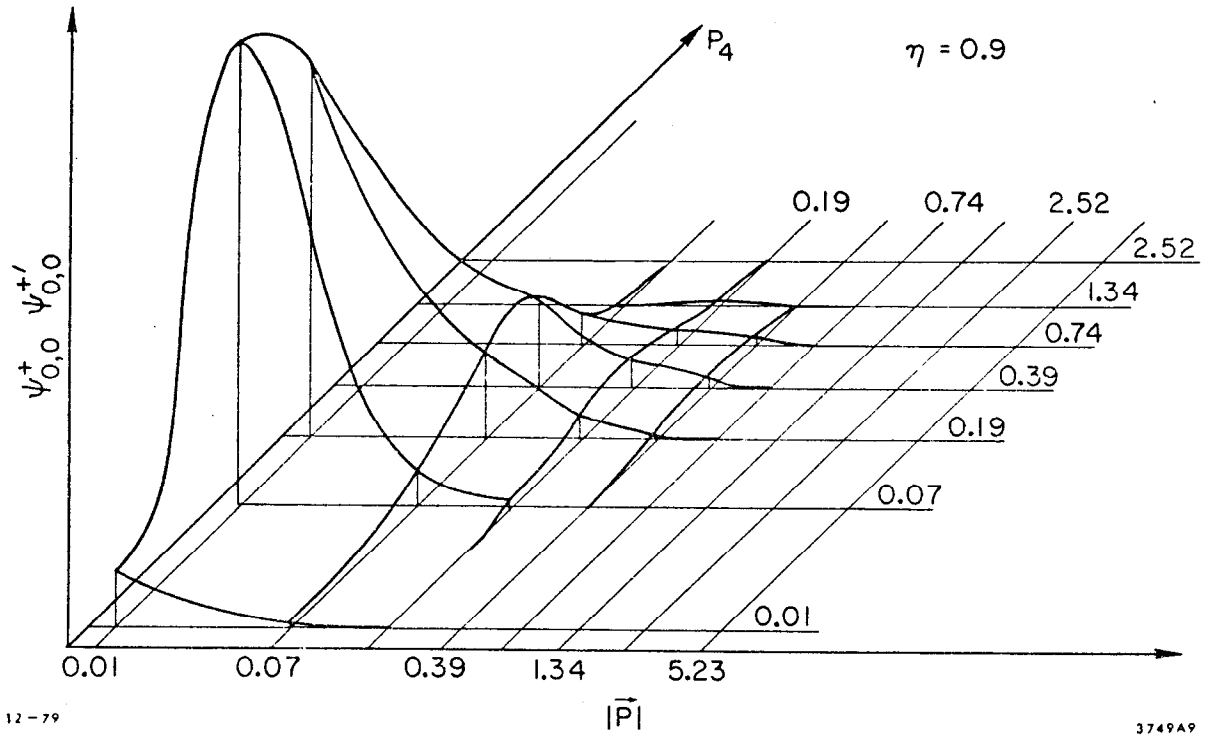
P_4
$\eta = 0.9$
0.19
0.74
2.52
2.52
1.34
0.74
0.39
0.19
0.07
0.01
$\psi^+_{0,0}$ $\psi^{+\prime}_{0,0}$
0.01
0.07
0.39
1.34
5.23
$|\vec{P}|$
12-79
3749A9

Fig. 9

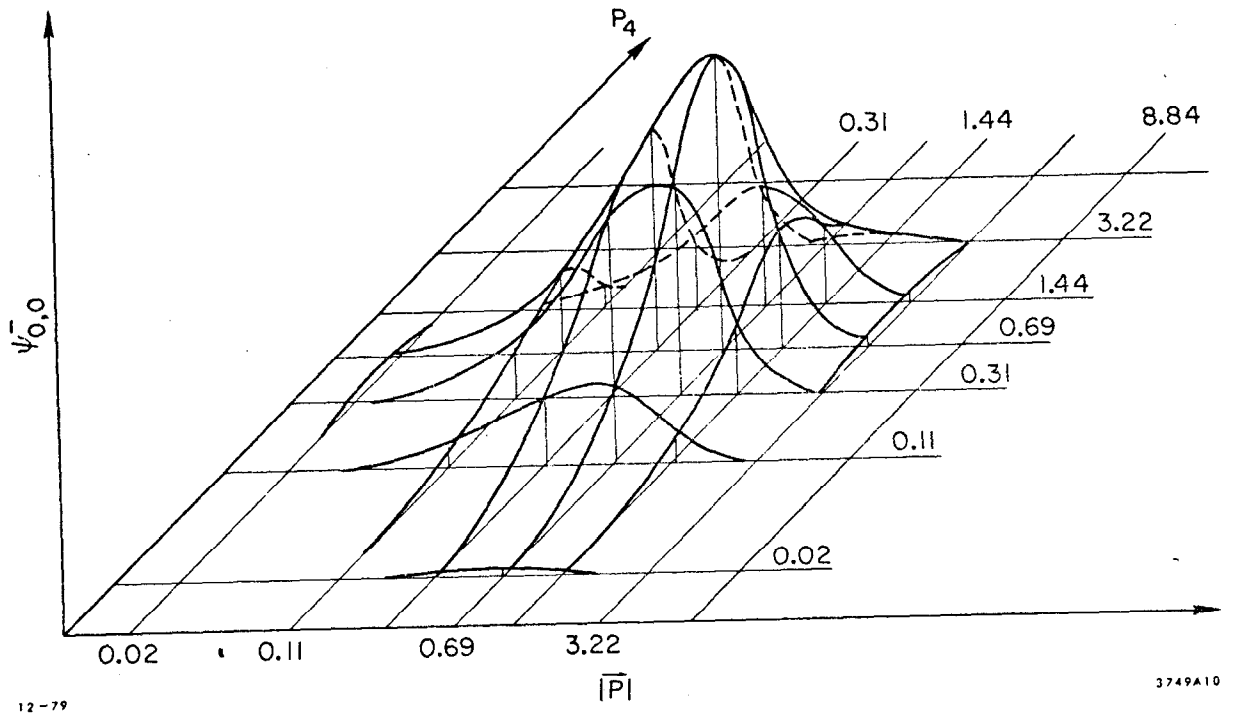
P4
0.31
1.44
8.84
3.22
1.44
0.69
0.31
0.11
0.02
0.02
0.11
0.69
3.22
|P|
12-79
3749A10

Fig. 10

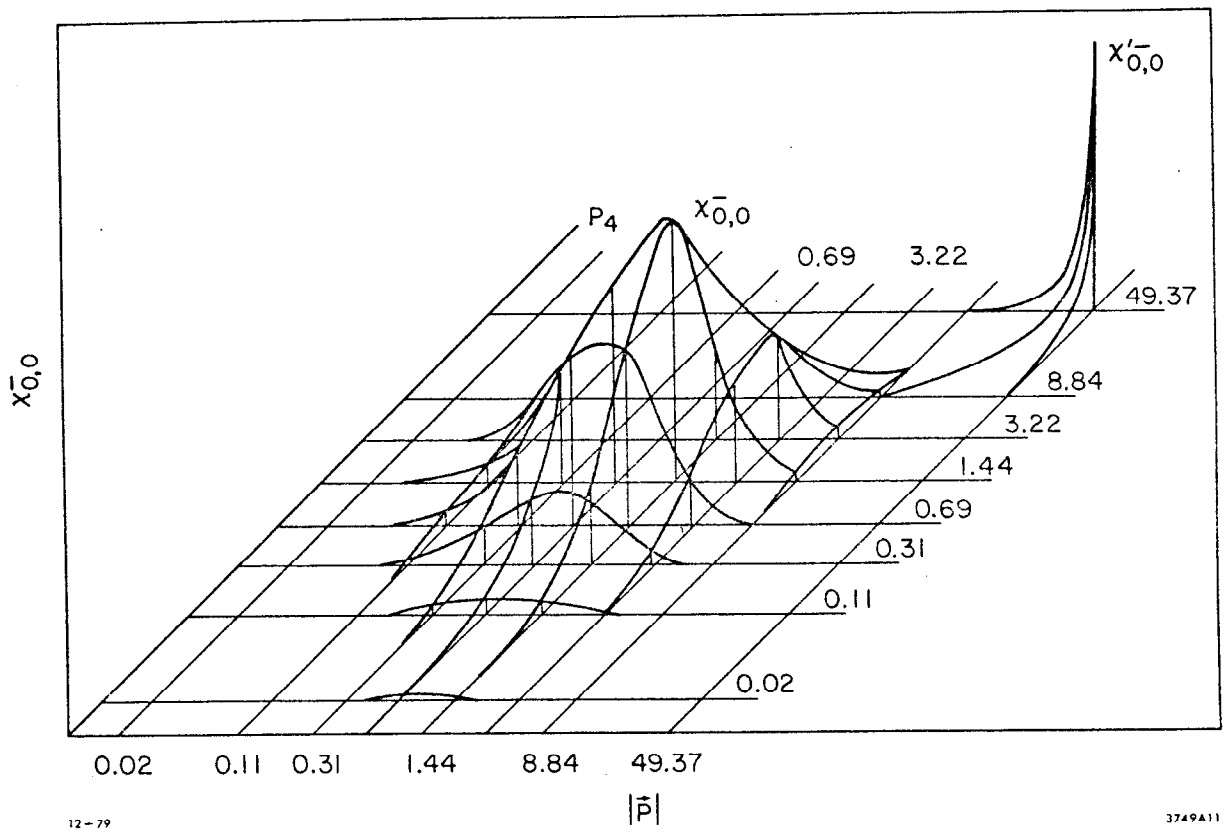
$X'^{-}_{0,0}$
P_4
$X^{-}_{0,0}$
0.69
3.22
49.37
8.84
3.22
1.44
0.69
0.31
0.11
0.02
$X^{-}_{0,0}$
0.02
0.11
0.31
1.44
8.84
49.37
$|\vec{P}|$
12-79
3749A11

Fig. 11